



PSO based neuro fuzzy sliding mode control for a robot manipulator

M. Vijay, Debashisha Jena*

Department of Electrical Engineering, NITK, Surathkal, Mangalore 575025, India

Received 15 August 2015; received in revised form 27 May 2016; accepted 23 August 2016

Abstract

This paper presents the control strategy of two degrees of freedom (2DOF) rigid robot manipulator based on the coupling of artificial neuro fuzzy inference system (ANFIS) with sliding mode control (SMC). Initially SMC with proportional integral derivative (PID) sliding surface is adapted to control the robot manipulator. The parameters of the sliding surface are obtained by minimizing a quadratic performance indices using particle swarm optimization (PSO). Variations of SMC i.e. boundary sliding mode control (BSMC) and boundary sliding mode control with PID sliding surface (PIDBSMC) are developed for optimized performance index. Finally an ANFIS adaptive controller is proposed to generate the adaptive control signal and found to be more robust with regard to disturbances in input torque.

© 2016 Electronics Research Institute (ERI). Production and hosting by Elsevier B.V. This is an open access article under the CC BY-NC-ND license (<http://creativecommons.org/licenses/by-nc-nd/4.0/>).

Keywords: Robot manipulator; Optimal control; Sliding mode control; Adaptive control; Disturbance rejection; Position tracking

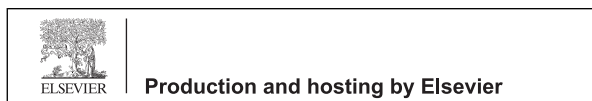
1. Introduction

Control of robotic systems is vital due to the wide range of their applications and this system is non-linear multi-input and multi-output (MIMO). The main objective of robot control systems is to follow a reference trajectory, which involves the generation of a control signal to make error between the robot position and reference to zero (Gracia et al., 2012). Non-linear control methodologies are more general because they can be used in linear and non-linear systems. These controllers can solve different problems with robustness i.e. invariance to system uncertainties and resistance to the external disturbances. The most common non-linear methodologies that have been proposed to solve the control problems are feedback linearization control, sliding mode control, adaptive control and artificial intelligence based methodology. SMC is the one of the best non-linear robust controllers to control robot manipulator, which has been analyzed by many researchers (Pilton and Sulaiman, 2012).

* Corresponding author.

E-mail addresses: mokenapalli.vijay@gmail.com (M. Vijay), bapu4002@gmail.com (D. Jena).

Peer review under the responsibility of Electronics Research Institute (ERI).



<http://dx.doi.org/10.1016/j.jesit.2016.08.006>

2314-7172/© 2016 Electronics Research Institute (ERI). Production and hosting by Elsevier B.V. This is an open access article under the CC BY-NC-ND license (<http://creativecommons.org/licenses/by-nc-nd/4.0/>).

Please cite this article in press as: Vijay, M., Jena, D., PSO based neuro fuzzy sliding mode control for a robot manipulator. J. Electr. Syst. Inform. Technol. (2016), <http://dx.doi.org/10.1016/j.jesit.2016.08.006>

This non-linear controller provides acceptable control performance with stability and robustness for non-linear systems (Jordanov and Surgenor, 1997; Slotine and Li, 1991; Utkin, 1992; Harashima et al., 1986). However, conventional SMC used in wide range has certain disadvantages. Firstly, chattering problem, this can cause high frequency oscillations in the controller output, secondly sensitivity to input disturbances and parameter uncertainties. Chattering phenomenon can cause some problems such as saturation and heat in mechanical parts of robot manipulators. To reduce or eliminate the chattering, various papers has been presented by many researchers and classify it into two methods: boundary layer saturation method and estimated uncertain method (Ertugrul and Kaynak, 1998; Curk and Jenermik, 2001; Khalil, 2002).

In recent years, artificial intelligence theory is being applied to SMC. Neural networks (NNs), Fuzzy logic and Neuro-fuzzy are combined with SMC and used in non-linear, time variant and uncertain plant. Some researchers applied fuzzy logic methodology in SMC to reduce the chattering (Barrero et al., 2002) and other researchers have applied sliding mode methodology in fuzzy logic controller (FLC) to improve the stability of system (Hang et al., 2003; Aloui et al., 2011). In Sun et al. (2011), the authors have addressed the robust trajectory tracking problem for a robot manipulator in the presence of uncertainties and disturbances. A neural network based sliding mode adaptive control (NNSMAC) which is a combination of sliding mode technique, neural network approximation and adaptive technique is designed for trajectory tracking of the robot manipulator. Authors, in Lin and Lenk (2008), Moradi and Malekizade (2013) and Rossomando et al. (2013) developed a design method of recurrent fuzzy neural networks (RFNN) control system for MIMO non-linear dynamic system. In (Guoling et al., 2014), the authors have addressed hybrid terminal sliding mode surfaces and a new fast decoupled terminal sliding mode control (FDTSMC) scheme.

The application of adaptive neural networks to robot manipulator is presented in Perez et al. (2012) which explain recurrent neural networks and Lyapunov function methodology. An adaptive type-2 FLC for flexible-joint manipulators with structured and unstructured dynamical uncertainties have introduced in (Chaoui et al., 2012). In Abdel et al. (2011), the author has proposed fuzzy partition to the state variables based on the Lyapunov synthesis. Authors in Zeinali and Notash (2010) and Ho et al. (2009) have presented a methodology that enables the designer to systematically derive the rule base of the control. In Kohrt et al. (2013), authors have discussed on-line robust control for robot manipulator.

This paper presents a new adaptive SMC for 2DOF robot manipulator; an adaptive tracking controller with a PID sliding surface. The adaptive SMC algorithm can estimate the value of switching gain constant (K_w) and boundary layer thickness (φ) in real time. A PID sliding surface, instead of a conventional sliding surface is adopted. An adaptive PIDBSMC (APIDBSMC) that can handle different level of input torque disturbances is derived and the stability of the closed loop system is established. The numerical simulation is presented to verify the effectiveness of the proposed control scheme. It is seen that the proposed APIDBSMC scheme offers several advantages such as the consistent estimation of K_w and φ large robustness to parameter variation and external disturbance. The remainder of this paper is organized as follows: Section 2 presents a description of robot manipulator, Section 3 presents the design and stability analysis of SMC controller, Section 4 presents ANFIS, Section 5 presents simulation results and discussions, and Section 6 summarizes the conclusions and contribution of work.

2. Description of robot manipulator

Dynamic equation of robot manipulator with n -degree freedom is represented as follows:

$$D(q(t))\ddot{q}(t) + C(q(t), \dot{q}(t))\dot{q}(t) + G(q(t)) + F(q(t), \dot{q}(t)) = \tau(t) \quad (1)$$

where $q(t)$, $\dot{q}(t)$ and $\ddot{q}(t) \in R^n$ are the link position, velocity and acceleration vectors respectively. $D(q(t)) \in R^{n \times n}$ is a symmetric positive definite inertia matrix, $C(q(t), \dot{q}(t))\dot{q}(t) \in R^n$ express the centrifugal forces, $G(q(t)) \in R^n$ denotes the gravity force, $F(q(t), \dot{q}(t)) \in R^n$ include the friction terms, external disturbances and $\tau(t)$ is total input control torque to the robot manipulator (Spong and Vidyasagar, 2004).

Dynamic equation (1) can be written as:

$$\ddot{q}(t) = D^{-1}(q(t))(\tau(t) - [C(q(t), \dot{q}(t))\dot{q}(t) + G(q(t)) + F(q(t), \dot{q}(t))]) \quad (2)$$

3. Controller design and stability analysis

3.1. PID optimal controller design for robot manipulator

The PID controller equation can be described as:

$$u(t) = K_p e(t) + K_i \int e(t) dt + K_d \frac{d}{dt} e(t) \quad (3)$$

where the error $e(t)$ is (desired path ($q_d(t)$) – actual path ($q(t)$)), K_p is $n \times n$ positive proportional gain matrix, K_i is $n \times n$ positive integral gain matrix and K_d is a $n \times n$ positive derivative gain matrix parameters to be selected. For 2 DOF robot manipulator, $n = 2$ and $K_p = \text{diag} \{K_{p1}, K_{p2}\}$, $K_i = \text{diag} \{K_{i1}, K_{i2}\}$ and $K_d = \text{diag} \{K_{d1}, K_{d2}\}$. The PID controller should provide a sufficient degree of stability for disturbances in input torque. The integral of position error should be minimized with different optimal control strategies (Tarokh and Zhang, 2014; Liu and Li, 2014). The system optimum parameters depend on the definition of optimality. The main function of a feedback control system is to minimize the objective function J given in Eq. (4).

$$J = \int_0^{\infty} t^b [e(t)]^m dt \quad (4)$$

where J is the objective function value; $e(t)$ is the error of position signal. Normally $m = 2$, $b = 0, 1$ and 2 represents three different optimum criterion Integral square error (ISE), Integral square time weighted error (ISTE) and Integral square time-squared weighted error (IST²E) respectively. The same Eq. (4) can be used to derive Integral absolute time error (IATE) by taking $m = 1$ and $b = 1$. Mean square of tracking error can be arbitrarily small by choosing appropriate design parameters (Ayoubi and Tai, 2012). In optimal control design the controller parameters are obtained by minimizing certain predefined performance indices. These performance indices can be ISE, ISTE, IATE, IST²E or any user defined function as is taken in case of linear quadratic regulator (LQR). Usually conventional local search algorithm such as gradient decent, conjugate gradient decent etc. are used to minimize the given predefined performance indices. However, the convergence of this gradient based algorithms highly dependent on initial search point at the same time there is a chance that the solution may get trapped by a local minimum, especially for a multi performance index. These limitations of conventional local search can be addressed by the use of global search algorithms such as evolutionary computation (EC), genetic algorithm (GA), particle swarm optimization (PSO) or any other derivative free algorithms.

In this paper PSO is taken into consideration to minimize the objective function. PSO is used to find the parameters such as PID parameters (K_p, K_i, K_d) and sliding control parameters (K_w, λ, ϕ) of different controllers discussed in the paper.

1. Finding the optimal PID parameters K_p, K_i , and K_d of the conventional PID controller.
2. Calculating the optimal parameters λ, K_w and ϕ of SMC and BSMC controllers.
3. Calculating the optimal parameters K_p, K_i, K_d, K_w and ϕ of PIDBSMC controller.

The method is based on a simplified social model, which is closely tied to the swarm theorem. The algorithm was introduced by Kennedy and Elberhart in 1995. Particle swarm optimization uses the velocity vector of each particle to update the position of each particle in the swarm (Liu and Wu, 2014).

The velocity of each particle based on the following Eq. (5) and defined as:

$$v_{k+1}^i = C[wv_k^i + c_1 r_1 (P^i - x_k^i) + c_2 r_2 (p_k^g - x_k^i)] \quad (5)$$

where w is called inertial weight, p^i is the best position of particle i , p_k^g is the best position in the swarm k . The coefficients c_1 and c_2 are called cognitive and social parameters respectively. The r_1 and r_2 are random numbers between 0 and 1. Inertial weight under PSO is defined as $w = 0.5 \times (Z_r) + 0.5 \times (rand)$ where $Z_r = 4 \times (rand) \times (1 - rand)$.

3.2. Design of sliding mode controller (SMC)

SMC is one of the influential non-linear controllers for linear and non-linear systems. It provides a methodological solution for two main important controller challenges, i.e. stability and robustness (Amer et al., 2011).

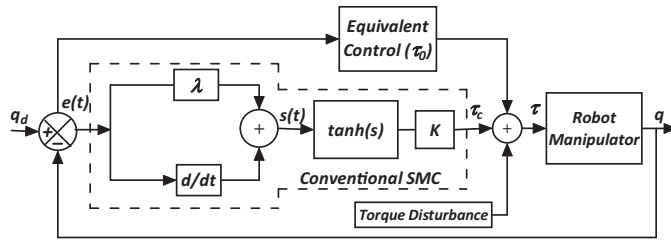


Fig. 1. Block diagram of conventional sliding mode control to robot manipulator.

3.2.1. Conventional sliding mode controller

The block diagram of conventional SMC is shown in Fig. 1. Total input control torque ($\tau(t)$) to the robot manipulator is defined as:

$$\tau(t) = \tau_0(t) + \tau_c(t) \tag{6}$$

where $\tau_0(t)$ is the equivalent control torque and $\tau_c(t)$ is the sliding mode control torque.

A time varying sliding surface $s(t)$ is given by the following Eq. (7) and defined as:

$$s(t) = \dot{e}(t) + \lambda e(t) \tag{7}$$

where ‘ λ ’ is positive constant, the main aim of this method is to keep $s(t)$ near to zero. The purpose of sliding mode control law is to force the tracking error $e(t)$ to approach the sliding surface and move along the sliding surface to the origin. Therefore, sliding surface should be stable, which means the error dies out asymptotically. This implies that the system dynamics tracks the desired trajectory.

The derivative of sliding surface with respect to time can be expressed as follows:

$$\dot{s}(t) = \ddot{e}(t) + \lambda \dot{e}(t) \tag{8}$$

$$\dot{s}(t) = \ddot{q}_d(t) - \ddot{q}(t) + \lambda \dot{e}(t) \tag{9}$$

where $\ddot{e}(t) = \ddot{q}_d(t) - \ddot{q}(t)$ and substituting the value of $\ddot{q}(t)$ from Eq. (2) in Eq. (9) gives as:

$$\dot{s}(t) = \ddot{q}_d(t) + \lambda \dot{e}(t) - D^{-1}(q(t))[\tau(t) - [C(q(t), \dot{q}(t))\dot{q}(t) + G(q(t)) + F(q(t), \dot{q}(t))]] \tag{10}$$

The control effort is derived from the solution of $\dot{s}(t) = 0$. This control effort is known as equivalent control effort represented by $\tau_0(t)$, which is required to achieve the desired trajectory tracking without considering disturbances and uncertainties.

$$\dot{s}(t) = \ddot{q}_d(t) + \lambda \dot{e}(t) - D^{-1}(q(t))[\tau_0(t) - [C(q(t), \dot{q}(t))\dot{q}(t) + G(q(t)) + F(q(t), \dot{q}(t))]] = 0 \tag{11}$$

$$\tau_0(t) = D(q(t))(\ddot{q}_d(t) + \lambda \dot{e}(t)) + C(q(t), \dot{q}(t))\dot{q}(t) + G(q(t)) + F(q(t), \dot{q}(t)) \tag{12}$$

However, if unpredictable disturbances or uncertainties occur, the equivalent control effort ($\tau_0(t)$) cannot ensure the favorable control performance. Therefore, auxiliary control effort should be designed to eliminate the effect of the unpredictable disturbances. Finally, the sliding surface should be stable, which means the error dies out asymptotically. The Lyapunov like Lemma is used to prove the stability of the designed control system.

The Lyapunov stability function is defined as:

$$V(t) = \frac{1}{2} s^T(t) s(t) \tag{13}$$

A sufficient condition, which gives the guarantee that the tracking position error will translate from reaching phase to sliding phase is also known as the reaching condition and expressed in Eq. (14).

$$\dot{V}(t) = s^T(t) \dot{s}(t) < 0, \quad s(t) \neq 0 \tag{14}$$

To obtain the reaching control signal, Eq. (14) can be defined as:

$$\begin{aligned} \dot{V}(t) = & s^T(t)[\ddot{q}_d(t) + \lambda\dot{e}(t) - D^{-1}(q(t))[\tau_0(t) + \tau_c(t)] - D^{-1}(q(t))[C(q(t), \dot{q}(t))\dot{q}(t) \\ & + G(q(t)) + F(q(t), \dot{q}(t))] \end{aligned} \quad (15)$$

Substituting Eq. (12) into Eq. (15), we get as:

$$\begin{aligned} \dot{V}(t) = & s^T(t)[\ddot{q}_d(t) + \lambda\dot{e}(t) - D^{-1}(q(t))[D(q(t))(\ddot{q}_d(t) + \lambda\dot{e}(t)) + C(q(t), \dot{q}(t))\dot{q}(t) + G(q(t)) + F(q(t), \dot{q}(t)) \\ & + \tau_c(t)] - D^{-1}(q(t))[C(q(t), \dot{q}(t))\dot{q}(t) + G(q(t)) + F(q(t), \dot{q}(t))] \end{aligned} \quad (16)$$

$$\dot{V}(t) = s^T(t)\dot{s}(t) = -s^T(t)D^{-1}(q(t))\tau_c(t) \quad (17)$$

To ensure $s^T(t)\dot{s}(t) < 0$, the reaching control law is selected as:

$$\tau_c(t) = D(q(t))K_w \text{sign}(s(t)) \quad (18)$$

Substituting Eq. (18) into Eq. (17), then the Lyapunov stability condition becomes as:

$$\dot{V}(t) < -s^T(t)D^{-1}(q(t))D(q(t))K_w \text{sign}(s(t)) \quad (19)$$

$$\dot{V}(t) < -K_w s^T(t) \text{sign}(s(t)) \quad (20)$$

$$\dot{V}(t) < -K_w |s(t)| \quad (21)$$

where $|s(t)| = s^T(t) \text{sign}(s(t))$.

The ‘*sign*’ function, which is used in Eq. (18) creates more chattering effect on the control torque. In order to avoid the chattering effect, the ‘*sign*’ function is replaced by the ‘*tanh*’ (hyperbolic tangent) function and expressed in Eq. (22).

$$\dot{V}(t) < -K_w s^T(t) \tanh(s(t)) \quad (22)$$

The term ‘ $s^T(t)\tanh(s(t))$ ’ in Eq. (22) is always positive, so that the entire equation becomes negative provided that $s(t)$ satisfies the following conditions.

1. If $s(t)$ is positive and $\tanh(s(t))$ is also positive then $s^T(t)\tanh(s(t))$ is always positive.
2. If $s(t)$ is negative and $\tanh(s(t))$ is also negative then $s^T(t)\tanh(s(t))$ is always positive.

Finally, the reaching control torque ($\tau_c(t)$) is given in Eq. (23) and follows as:

$$\tau_c(t) = D(q(t))K_w \tanh(\dot{e}(t) + \lambda e(t)) \quad (23)$$

where $K_w = \text{diag}\{K_{w1}, K_{w2}\}$ and it represents reaching control gain matrix with upper bound of uncertainties. Tuning positive time constant K_w given Eq. (23) is one of the most important challenges in conventional sliding mode control. Based on discontinuous part the chattering phenomenon can lead to oscillations in the output. To reduce the chattering effect, the boundary layer method is used. In boundary layer method the basic idea is to replace the discontinuous function by a smooth saturation function near to a small neighborhood of the switching surface. This replacement causes an increase in performance error. Therefore, to compensate the error performance an updated control is needed. In this work the saturation function is considered as given in Eq. (24).

$$\text{sat} \left(\frac{s(t)}{\varphi(t)} \right) = \begin{cases} \tanh \left(\frac{s(t)}{\varphi(t)} \right), & \text{for } \left| \frac{s(t)}{\varphi(t)} \right| \geq 1; \\ \frac{s(t)}{\varphi(t)}, & \text{for } \left| \frac{s(t)}{\varphi(t)} \right| \leq 1; \end{cases} \quad (24)$$

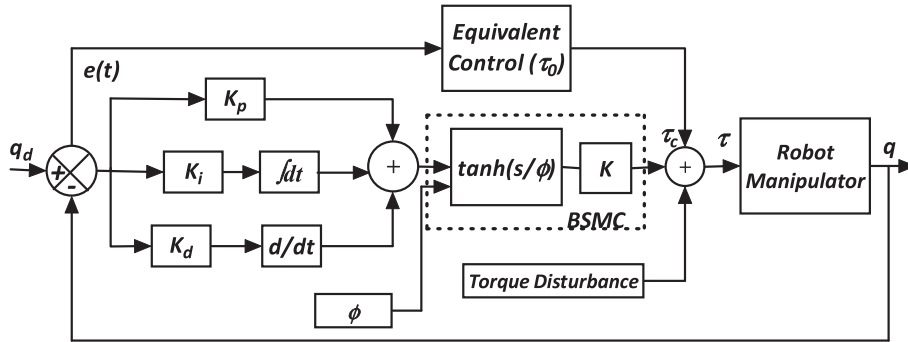


Fig. 2. Block diagram of the SMC with PID sliding surface to robot manipulator.

Finally the SMC control law with boundary layer (BSMC) becomes as:

$$\tau_c(t) = K \tanh \left(\frac{\dot{e}(t) + \lambda e(t)}{\phi(t)} \right) \quad (25)$$

where K is defined as the positive gain matrix and it is defined as $K = D(q(t))K_w$.

3.2.2. SMC with PID sliding surface and stability analysis

Fig. 2 shows the block diagram for SMC control of robot manipulator with the PID sliding surface. In SMC, it is very important to implement sliding surface $s(t)$ which is expected to provide desired control specifications and performance. The trajectories are enforced to lie on the sliding surface.

The PID sliding surface of tracking error is defined as:

$$s(t) = K_p e(t) + K_i \int e(t) dt + K_d \frac{de(t)}{dt} \quad (26)$$

The derivative of the sliding surface with respect to time is expressed as:

$$\dot{s}(t) = K_p \dot{e}(t) + K_i e(t) + K_d \ddot{e}(t) \quad (27)$$

$$\dot{s}(t) = K_p \dot{e}(t) + K_i e(t) + K_d (\ddot{q}_d(t) - \ddot{q}(t)) \quad (28)$$

Substituting the Eq. (2) into Eq. (28), we get as:

$$\dot{s}(t) = K_p \dot{e}(t) + K_i e(t) + K_d (\ddot{q}_d(t) - (D^{-1}(q(t))(\tau(t) - [C(q(t), \dot{q}(t))\dot{q}(t) + G(q(t)) + F(q(t), \dot{q}(t))])))) \quad (29)$$

The control effort is derived as the solution of $\dot{s}(t) = 0$, without the uncertainties to achieve the desired performance under nominal model is referred as equivalent control effort, represented by $\tau_0(t)$.

$$\dot{s}(t) = K_p \dot{e}(t) + K_i e(t) + K_d (\ddot{q}_d(t) - (D^{-1}(q(t))(\tau_0(t) - [C(q(t), \dot{q}(t))\dot{q}(t) + G(q(t)) + F(q(t), \dot{q}(t))])))) = 0 \quad (30)$$

$$K_d D^{-1}(q(t))\tau_0(t) = K_p \dot{e}(t) + K_i e(t) + K_d \ddot{q}_d(t) + K_d D^{-1}(q(t)) - D^{-1}(q(t))[C(q(t), \dot{q}(t))\dot{q}(t) + G(q(t)) + F(q(t), \dot{q}(t))]] \quad (31)$$

$$\tau_0(t) = K_d^{-1} K_p D(q(t))\dot{e}(t) + K_d^{-1} K_i D(q(t))e(t) + D(q(t))\ddot{q}_d(t) + [C(q(t), \dot{q}(t))\dot{q}(t) + G(q(t)) + F(q(t), \dot{q}(t))]] \quad (32)$$

However, in case of unprintable disturbances or uncertainties, the equivalent control effort cannot ensure the favorable control performance. Therefore, auxiliary control effort should be designed to eliminate the effect of the unpredictable disturbance. For this purpose, the Lyapunov function can be chosen as:

$$V(t) = \frac{1}{2}s^T(t)s(t) \tag{33}$$

The reaching condition can be defined as:

$$\dot{V}(t) = s^T(t)\dot{s}(t) < 0, \quad s(t) \neq 0 \tag{34}$$

To obtain the reaching control signal for SMC with PID sliding surface controller is $\tau_c(t)$ can defined as:

$$\dot{V}(t) = s^T(t)\dot{s}(t) = s^T(t)[K_p\dot{e}(t) + K_i e(t) + K_d\ddot{e}(t)] \tag{35}$$

$$\begin{aligned} \dot{V}(t) = s^T(t)[K_p\dot{e}(t) + K_i e(t) + K_d(\ddot{q}_d(t) - D^{-1}(q(t))(\tau_0(t) + \tau_c(t) - [C(q(t), \dot{q}(t))\dot{q}(t) + G(q(t)) \\ + F(q(t), \dot{q}(t))]))] \end{aligned} \tag{36}$$

Substituting Eq. (32) into Eq. (36), we get as:

$$\begin{aligned} \dot{V}(t) = s^T(t)[K_p\dot{e}(t) + K_i e(t) + K_d(\ddot{q}_d(t) - D^{-1}(q(t))(K_d^{-1}K_pD(q(t))\dot{e}(t) + K_d^{-1}K_iD(q(t))e(t) \\ + D(q(t))\ddot{q}_d(t) + [C(q(t), \dot{q}(t))\dot{q}(t) + G(q(t)) + F(q(t), \dot{q}(t))] + \tau_c(t) - [C(q(t), \dot{q}(t))\dot{q}(t) \\ + G(q(t)) + F(q(t), \dot{q}(t))])] \end{aligned} \tag{37}$$

$$\dot{V}(t) = -s^T(t)K_dD^{-1}(q(t))\tau_c(t) \tag{38}$$

To ensure $s^T(t)\dot{s}(t) < 0$, the reaching control law should be selected as:

$$\tau_c(t) = D(q(t))K_d^{-1}K_w \text{sign}(s(t)) \tag{39}$$

$$\tau_c(t) = K \text{sign}(s(t)) \tag{40}$$

where $K = D(q(t))K_d^{-1}K_w$ and K_w is reaching control gain of sliding mode controller. Obviously, substituting Eq. (39) into Eq. (38), then we get as:

$$\dot{V}(t) < -s^T(t)K_dD^{-1}(q(t))K_d^{-1}D(q(t))K_w \text{sign}(s(t)) \tag{41}$$

$$\dot{V}(t) < -K_w s^T(t) \text{sign}(s(t)) \tag{42}$$

In order to avoid chattering effect, the ‘sign’ function in Eq. (39) is replaced by ‘tanh’ (hyper tangent) function.

$$\dot{V}(t) < -K_w s^T(t) \tanh(s(t)) \tag{43}$$

Similar to Eq. (22), we can prove stability condition for above given Eq. (43) also. Finally the reaching control signal $\tau_c(t)$ is given in Eq. (44) as follows:

$$\tau_c(t) = K \tanh\left(\frac{K_p e(t) + K_i \int e(t)dt + K_d(de(t)/dt)}{\varphi(t)}\right) \tag{44}$$

4. Adaptive PIDBSMC design and stability analysis

In ANFIS using a given input/output data set, the tool box function constructs a fuzzy inference system (FIS) whose membership function are tuned (adjusted) using either a back propagation algorithm alone or in a combination with the least square type of method. Both artificial neural networks (ANN) and fuzzy logics are used in architecture. In the process of developing the ANFIS adaptive controller, the training was performed on the MATLAB environment by using ANFIS topologies under various input membership functions with various training data set under different

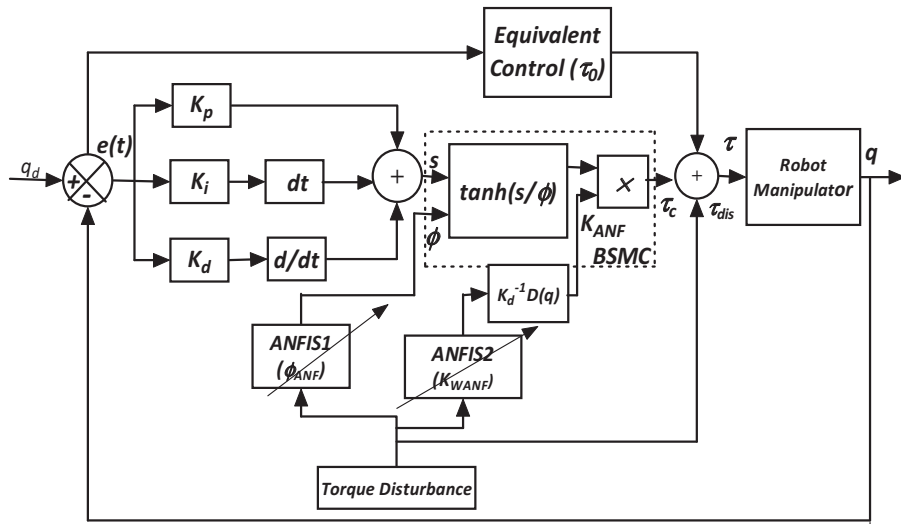


Fig. 3. Block diagram of the ANFIS adaptive BSMC with PID sliding surface to the robot manipulator.

Table 1
 Obtained results of the used membership function for each of the inputs.

Sl. no	Used membership function	Training error values K_{WANF}	Training error values for φ_{ANF}
1	gaussmf	3.087e-3	3.27e-7
2	gauss2mf	3.007e-3	2.23e-7
3	primf	3.095e-3	4.31e-7
4	dsimf	3.156e-3	3.48e-7
5	psigmf	3.146e-3	3.48e-7
6	gbellmf	0.09923	2.47e-7
7	trimf	3.25e-3	3.18e-7
8	trapmf	3.112e-3	3.51e-7

disturbance conditions. Fig. 3 shows a block diagram of the ANFIS adaptive BSMC with PID sliding surface to the robot manipulator.

Similar to Eq. (26), the sliding surface for adaptive PIDBSMC can be defined as:

$$s(t) = K_p e(t) + K_i \int e(t) dt + K_d \frac{de(t)}{dt} \quad (45)$$

From the Eq. (34), we can define the necessary conditions for Lyapunov stability as:

$$\dot{V}(t) = s^T(t) \dot{s}(t) < 0, \quad s(t) \neq 0 \quad (46)$$

The stability of APIDBSMC can be proved from Eq. (43)

$$\dot{V}(t) < -s^T(t) \tanh(s(t)) \quad (47)$$

Finally, we can define the final control law developed by APIDBSMC is defined as:

$$\tau_c(t) = K_{ANF} \tanh \left(\frac{K_p e(t) + K_i \int e(t) dt + K_d (de(t)/dt)}{\varphi_{ANF}(t)} \right) \quad (48)$$

where $K_{ANF} = (K_{WANF}) K_d^{-1} D(q(t))$ and $K_{WANF} = \{K_{WANF1}, K_{WANF2}, \dots, K_{WANFn}\}$ is adaptive switching is gain matrix and φ_{ANF} is the boundary layer thickness of sliding mode controller.

From the Table 1, it is observed that gauss2mf provides minimum training error for both cases. Finally the gauss2mf membership function used for designing of ANFIS network for SMC. Fig. 3 illustrates the framework of the ANFIS

adaptive BSMC with PID sliding surface. Here ANFIS model provides adaptive K_{WANF} and φ_{ANF} to the BSMC for different torque disturbance conditions.

5. Results and discussion

Simulation is carried out for the 2DOF robot manipulator in MATLAB and SIMULINK. Initially the optimum robot manipulator controller is designed for IATE, ISE and ISTE control strategies for different torque disturbance conditions. Results are obtained by tuning the parameters through a global search algorithm, i.e. PSO under various input torque disturbance conditions.

Tables 2 and 3 show the conventional PID control tuning parameters resulted from PSO with IATE, ISE and ISTE control strategies for 5% and 10% disturbances. From above tables, it is observed that the model with ISTE control strategy gives minimum objective function values (i.e. 0.0168 and 0.0313 for 5% and 10% disturbances in input torque respectively) compared to IATE and ISE optimal control strategies. Finally ISTE control strategy has selected for further simulation works of robot manipulator. Table 4 shows the SMC parameters and objective function values for 5%, 7.5% and 10% torque disturbances resulting from PSO. Table 5 shows the BSMC parameters and objective function values for 5%, 7.5% and 10% torque disturbances resulting from PSO.

Figs. 4 and 5 show the response of robot manipulator link positions for 10% disturbance in input torque with ISTE optimum criterion under PID, SMC and BSMC methods.

The maximum operating torque (τ) under 10% input torque disturbance is $0.8 \times 10e4$ N m. For a 10% disturbance of input torque (i.e. 800 N m) the PID parameters obtained from PSO tuning of PIDBSMC are found to be, $K_{p1} = 734.5$, $K_{i1} = 780.2$, $K_{d1} = 461.3$, $K_{p2} = 742.2$, $K_{i2} = 786.4$ and $K_{d2} = 106.1$ as given in Table 6.

Table 2
 PID tuning parameters and objective function values for 5% input torque disturbance.

Sl. no	Controlling parameters	IATE	ISE	ISTE
1	K_{p1}	514.5	819.5	532.8
2	K_{i1}	156.6	574.8	217.8
3	K_{d1}	42.55	459.9	168.7
4	K_{p2}	204.7	119.73	686.7
5	K_{i2}	318.8	257.6	329.7
6	K_{d2}	901.3	40.21	164.8
	Objective function value (J)	0.5147	0.0180	0.0168

Table 3
 PID tuning parameters and objective function values for 10% disturbance in input torque.

Sl. no	Controlling parameters	IATE	ISE	ISTE
1	K_{p1}	814.9	665.6	814.9
2	K_{i1}	631.5	799.5	631.5
3	K_{d1}	745.1	122.1	745.1
4	K_{p2}	380.2	416.7	380.2
5	K_{i2}	427.6	716.5	427.6
6	K_{d2}	169.7	777.6	427.6
	Objective function value (J)	0.5506	0.09713	0.0313

Table 4
 SMC parameters for 5%, 7.5% and 10% of input torque disturbances.

Sl. no	Parameters of SMC	5% disturbance	7.5% disturbance	10% disturbance
1	K_w	297.1	178.3932	315.7
2	λ	57.42	550.8505	9.25
	Objective function value (J)	0.0009	0.00058	0.0073

Table 5
 BSMC parameters for 5%, 7.5% and 10% of input torque disturbances.

Sl. no	Parameters of SMC	5% disturbance	7.5% disturbance	10% disturbance
1	K_w	454.25	634.8768	589.03
2	λ	934.49	816.5764	870.44
3	ϕ	0.3858	0.5959	0.0842
	Objective function value (J)	3.386e-6	5.5e-6	6.742e-7

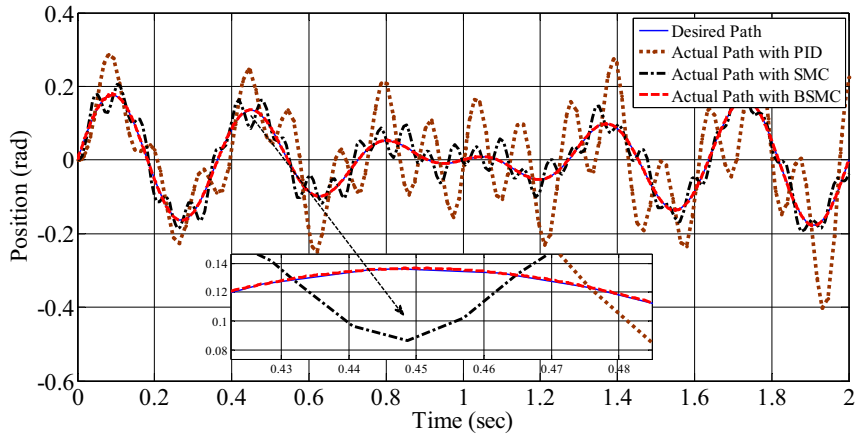


Fig. 4. Tracking positions of Link 1 with PID, SMC and BSMC for 10% disturbance in input torque.

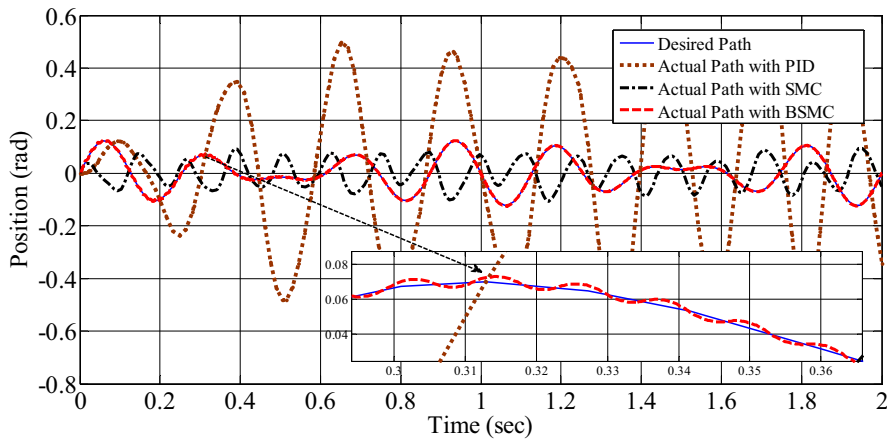


Fig. 5. Tracking positions of Link 2 with PID, SMC and BSMC for 10% disturbance in input torque.

Table 6
 BSMC with PID sliding surface parameters for 5%, 7.5% and 10% of input torque disturbance.

Sl. no	Controlling parameters	5% disturbance	7.5% disturbance	10% disturbance
1	K_{p1}	870.5	439.8	734.5
2	K_{i1}	265.5	217.5	780.2
3	K_{d1}	573.7	533.1	461.3
4	K_{p2}	411.9	831.4	747.2
5	K_{i2}	36.9	450.4	786.4
6	K_{d2}	490.4	600.9	106.1
7	K_w	662.6	766.2	992.9
8	ϕ	0.5215	0.4978	0.1709
	Objective function value (J)	1.498e-8	3.437e-6	6.168e-7

Table 7
Controlling parameters from PSO and ANFIS.

Sl. no	Disturbance in input torque (%)	Parameters from PSO		Objective function value (J)	Parameters from ANFIS		Objective function value (J) for test data
		K	ϕ		K_{ANF}	ϕ_{ANF}	
1	1.75	913.5	0.381	2.45e-6	722.1	0.048	4.61e-4
2	2.85	962.8	0.755	6.01e-6	924	0.022	4.25e-5
3	7.55	367.8	0.766	3.5e-5	1026	0.175	2.88e-5
4	9.35	699.7	0.763	3.49e-5	994.5	0.016	4.03e-6
5	10.82	602.8	0.487	4.09e-6	964.4	0.065	8.08e-6

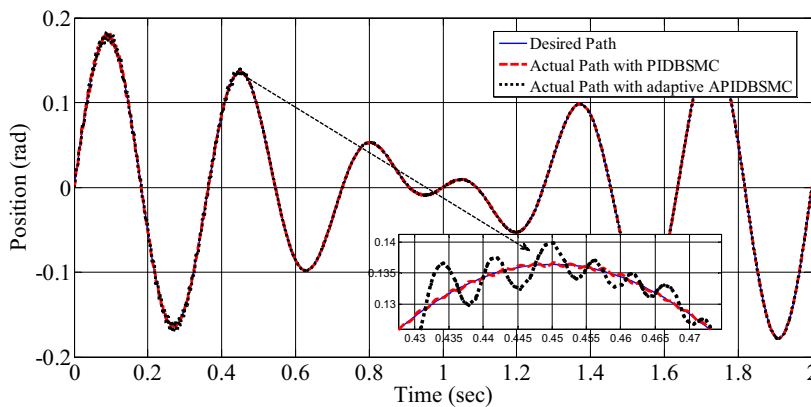


Fig. 6. Tracking positions of Link 1 with PIDBSMC and APIDBSMC for 10% disturbance in input torque.

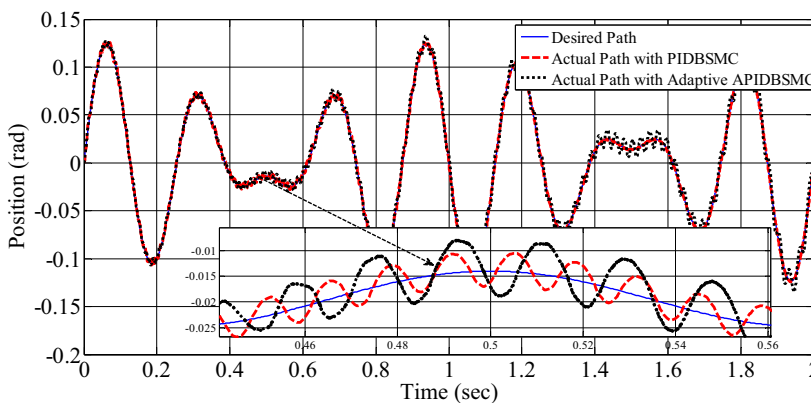


Fig. 7. Tracking positions of Link 2 with PIDBSMC and APIDBSMC for 10% disturbance in input torque.

These tuned PID parameters given are kept fixed for all iterations, but sliding mode control parameters (K_w and ϕ) are calculated by using PSO. For data generation K and ϕ are obtained for various disturbances ranging from 0% to 11% with a step size of almost 0.1% disturbance. Total 115 number of data (% of disturbance, K_w and ϕ) are collected by PIDBSMC tuned by PSO. Among those data, 110 data had been used for training and rest 5 data used for testing the ANFIS controller. Here K_{WANF} and ϕ_{ANF} are tuned for various input disturbances ranging from 0 to 11%. Finally results of the APIDBSMC controller are compared with PSO tuned PIDBSMC controller in Table 7.

Figs. 6 and 7 show the response of robot manipulator link positions for 10% disturbance in input torque with ISTE optimum criterion under PIDBSMC and APIDBSMC methods. From the figure it is clear that the tracking error is minimum for PIDBSMC compared to conventional PID, SMC and BSMC. Figs. 8 and 9 show control torque input by

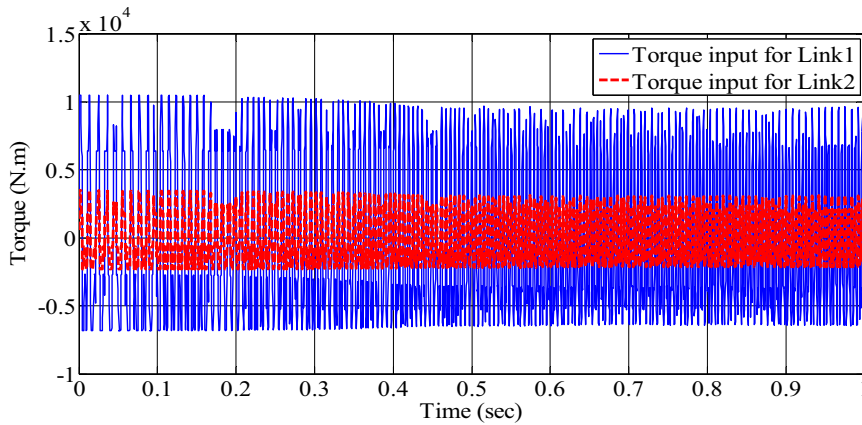


Fig. 8. Control input of Link1 and Link 2 using SMC proposed controller for 10% disturbance in input torque.

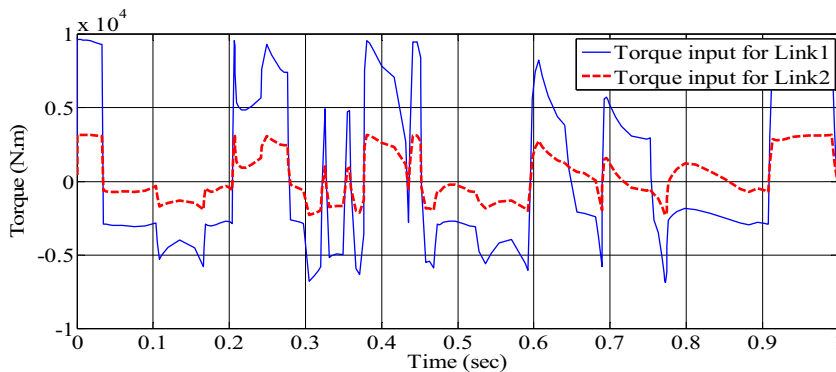


Fig. 9. Control input of Link1 and Link 2 using APIDBSMC proposed controller for 10% disturbance in input torque.

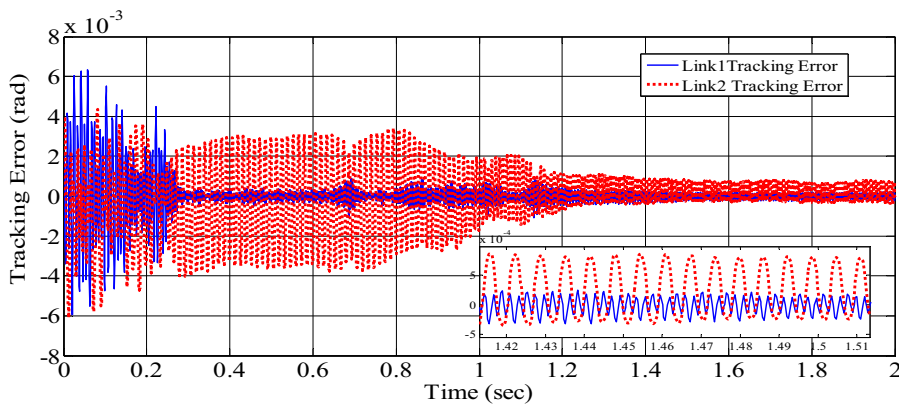


Fig. 10. Comparison of position tracking error responses between desired path and actual path with APIDBSMC for 10% disturbance in input torque.

using SMC and APIDBSMC proposed controllers. Fig. 10 shows the tracking error responses for 10% disturbance in input torque under PIDBSMC.

6. Conclusion

This paper discusses variation of SMC controller where the PID sliding surface is taken into consideration and controlling parameters are obtained by using PSO. The PSO is used to obtain the optimal PID parameters and sliding

control parameters where the objective function for PSO is taken as the IATE, ISE and ISTE. Control performance of BSMC and PIDBSMC compared in terms of tracking error, disturbance rejection and elimination of chattering for different torque disturbance. As PIDBSMC parameters are obtained from PSO tuning in offline, is not suitable for real time system. Finally, it is concluded that, ANFIS based PIDBSMC can be used for real time control of robot manipulator where sliding control parameters are changed adaptively for giving good control performance under different input disturbances. The stability of the control system is rigorously guaranteed by Lyapunov stability theorem. In the future work it will be interesting and challenging to develop a control algorithm for 3DOF robot manipulator with model parameter uncertainties and various disturbances in torque.

Appendix A. Parameters of 2DOF robot manipulator

Mass of Link 1 (m_1) = 10 kg, Mass of Link 2 (m_2) = 10 kg and Length of Link 1 (L_1) = 0.5 m, Length of Link 2 (L_2) = 0.5 m.

Appendix B. PSO parameters

Cognitive parameter (c_1) = 2, social parameter (c_2) = 2, $iter_{max}$ = 100, constriction factor (C) = 1, population size = 100, W_{max} = 0.9 and W_{min} = 0.217.

References

- Gracia, L., Garelli, F., Sala, A.A., 2012. Path condition method with trap avoidance. *Robot. Autom. Syst.* 60, 862–873.
- Pilton, P., Sulaiman, N.B., 2012. Review of sliding mode control of robot manipulator. *World Appl. Sci. J.* 18, 1855–1869.
- Iordanov, I.N., Surgenor, B.W., 1997. Experimental evaluation of robustness of discrete sliding mode control versus linear quadratic control. *IEEE Trans. Control Syst. Technol.* 5, 254–260.
- Slotine, J.J.E., Li, W., 1991. *Applied Non-linear Control*. Prentice-Hall Inc.
- Utkin, I.V., 1992. *Sliding Mode Control Optimization*. Springer-Verlag.
- Harashima, F., Hashimoto, H., Maruyama, K., 1986. Practical robust control of robot arm using variable structure system. In: *IEEE Int. Conference on Robotics and Automation*, pp. 532–539.
- Ertugrul, E., Kaynak, O., 1998. Neural computational the equivalent control in sliding mode for robot trajectory appliances. In: *IEEE Int. Conference on Robotics and Automation*, pp. 2042–2047.
- Curk, B., Jenermik, K., 2001. Sliding mode control with perturbation estimation: application on DD robot mechanism. *Robotica*, 641–648.
- Khalil, K.H., 2002. *Non-linear Systems*, 3rd ed. Prentice Hall.
- Barrero, F., Torralba, A., Gonazaler, A., Galven, E., 2002. Speed control of induction motors using a novel fuzzy sliding Structure. *IEEE Trans. Fuzzy Syst.* 10, 375–383.
- Hang, Z., Su, H., Chi, J., 2003. Adaptive sliding mode-like fuzzy logic control for high order nonlinear systems. In: *IEEE Conference on Intelligent Control*, pp. 788–792.
- Aloui, S., Pages, O., Hajiaji, A.E., Chaari, A., Koubaa, Y., 2011. Improved fuzzy sliding mode control for a class of MIMO non-linear uncertain and perturbed systems. *Appl. Soft Comput.* 11, 820–826.
- Sun, T., Pei, H., Pan, H., Zhou, H., 2011. Neural network based sliding mode adaptive control of robot manipulators. *Neurocomputing* 74, 377–2384.
- Lin, C.M., Lenk, C.H., 2008. Recurrent fuzzy neural network control for MIMO non-linear systems. *Intell. Autom. Soft Comput.* 14, 395–415.
- Moradi, M., Malekizade, H., 2013. Neural networks identification based multi-variable feedback linearization robust control for two link manipulator. *J. Intell. Robot. Syst.* 72, 167–178.
- Rossomando, F.G., Soria, C., Carelli, R., 2013. Sliding mode neuro adaptive control in trajectory tracking for mobile robots. *J. Intell. Robot. Syst.* 74, 931–944.
- Guoling, Z., Can, Z., Junting, C., 2014. Decoupled terminal sliding mode control for a class of under actuated mechanical systems with hybrid sliding surfaces. *Int. J. Innov. Comput.* 10, 2011–2023.
- Perez, J.J., Jose, P.D., Rogelio, S., 2012. Trajectory tracking error using PID control law for two-link robot manipulator via adaptive neural networks. In: *The Iberamerican Conference on Electronics Engineering and Computer Science Published in Procedia Technology*, vol. 3, pp. 139–146.
- Chaoui, H., Gueaieb, W., Biglarbegian, M., Mustappa, C.E., 2012. Computationally efficient adaptive type-2 fuzzy control flexible-joint manipulator. *Robotica* 2, 91–99.
- Abdel, B.S., Othaman, M.M., Khalis, A.M., 2011. A Robust fuzzy tracking control scheme for robot manipulators with experimental verification. *J. Intell. Control Autom.* 2, 100–111.
- Zeinali, M., Notash, L., 2010. Adaptive sliding mode control with uncertainty estimator for robot manipulator. *Mech. Mach. Theory* 45, 80–90.
- Ho, H.F., Wong, Y.K., Rad, A.B., 2009. Adaptive fuzzy sliding mode control with chattering elimination for non-linear SISO systems. *Simul. Model. Pract. Theory* 17, 1199–1210.
- Kohrt, C., Stamp, R., Pipe, A.G., Kiely, J., Schidmeir, G., 2013. An on-line robot trajectory planning and programming support systems for industrial use. *Robot. Comput.-Integr. Manuf.* 29, 71–79.

Spong, W., Vidyasagar, M., 2004. *Robot Dynamics and Control*. Wiley.

Tarokh, M., Zhang, X., 2014. Real time motion tracking of robot manipulators using adaptive genetic algorithm. *J. Intell. Robot. Syst.* 74, 697–708.

Liu, R., Li, S., 2014. Optimal integral sliding mode control scheme based on pseudo spectral method for robotic manipulators. *Int. J. Control* 87, 1131–1140.

Ayoubi, M.A., Tai, L.C., 2012. Intelligent control of a large variable speed wind turbine. *J. Sol. Energy Eng.* 134, 011001–11008.

Liu, Z.L., Wu, Y.Q., 2014. Modelling and adaptive tracking control for flexible joint robots with random noises. *Int. J. Control* 87, 2499–2510.

Amer, A.F., Sallam, E.A., Elawady, W.M., 2011. Adaptive fuzzy sliding mode control using supervisory fuzzy control for 3DOF planner robot manipulator. *Appl. Soft Comput.* 11, 4943–4953.